

Influence of biogenic pollen on optical properties of atmospheric aerosols observed by lidar over Gwangju, South Korea

Young Min Noh ^a, Detlef Müller ^{a,b,e,*}, Hanlim Lee ^c, Tae Jin Choi ^d

^a School of Environmental Science & Engineering, Gwangju Institute of Science & Technology (GIST), Republic of Korea

^b NASA Langley Research Center, VA, USA

^c Department of Atmospheric Sciences, Yonsei University, Republic of Korea

^d Department of Polar Climate Research, Korea Polar Research Institute (KOPRI), Republic of Korea

^e Leibniz Institute for Tropospheric Research, Leipzig, Germany

HIGHLIGHTS

- ▶ For the first time, optical properties of biogenic pollen were retrieved by lidar.
- ▶ Pollen particles were only detected during daytime within the PBL.
- ▶ Pollen particles result in the increase of aerosol optical depth.
- ▶ Pollen particles decrease the Ångström exponent of aerosol during pollen periods.
- ▶ The contribution of biogenic pollen to the total aerosol optical depth was 2–34%.

ARTICLE INFO

Article history:

Received 17 November 2012

Received in revised form

13 December 2012

Accepted 16 December 2012

Keywords:

Pollen

Lidar

Depolarization ratio

Optical depth

Ångström exponent

ABSTRACT

For the first time, optical properties of biogenic pollen, i.e., backscatter coefficients and depolarization ratios at 532 nm were retrieved by lidar observations. The extinction coefficient was derived with the assumption of possible values of the extinction-to-backscatter (lidar) ratio. We investigate the effect of the pollen on the optical properties of the observed atmospheric aerosols by comparing lidar and sun/sky radiometer measurements carried out at the lidar site. The observations were made with a depolarization lidar at the Gwangju Institute of Science & Technology (GIST) in Gwangju, Korea (35.13°N, 126.50°E) during an intensive observational period that lasted from 5 to 7 May 2009. The pollen concentration was measured with a Burkard trap sampler at the roof top of the Gwangju Bohoon hospital which is located 1 km away from the lidar site. During the observation period, high pollen concentrations of 1360, 2696, and 1952 m⁻³ day⁻¹ were measured on 5, 6, and 7 May, respectively. A high lidar depolarization ratio caused by biogenic pollen was only detected during daytime within the planetary boundary layer which was at 1.5–2.0 km height above ground during the observational period. The contribution of biogenic pollen to the total backscatter coefficient was estimated from the particle depolarization ratio. Average hourly values of pollen optical depth were retrieved by integrating the pollen extinction coefficients. We find average values of 0.062 ± 0.037 , 0.041 ± 0.028 and 0.067 ± 0.036 at 532 nm on 5, 6, and 7 May, respectively. The contribution of pollen optical depth to total aerosol optical depth was 2–34%. The sun/sky radiometer data show that biogenic pollen can affect optical properties of atmospheric aerosol by increasing aerosol optical depth and decreasing the Ångström exponent during daytime during the season of high pollen emission.

© 2012 Elsevier Ltd. All rights reserved.

1. Introduction

Airborne pollen is a form of biogenic air pollution and is recognized as one of the major agents of allergy-related diseases

such as asthma, rhinitis, and atopic eczema (Esch and Bush, 2003). These negative effects of airborne pollen on human health are increasing due to the impact of climate change on biota (Beggs, 2004; D'Amato and Cecchi, 2008; Shea et al., 2008). The onset of pollen transport and the duration of pollen emission in the air during the year may change due to temperature changes that in turn can cause a change in the time when plants grow (Frei, 1998; Teranishi et al., 2000). The intensity of pollen transport and

* Corresponding author. Leibniz Institute for Tropospheric Research, Leipzig, Germany. Tel.: +49 341 2717 7064; fax: +49 341 235 2361.

E-mail address: detlef@tropos.de (D. Müller).

changing patterns of pollen transport may be caused by changes in main wind directions. Precipitation events may reduce the concentration of pollen in the atmosphere as a result of wash-out of pollen in the planetary boundary layer (PBL). The type of pollen can change, too, as the type of trees and grass that grow in various regions may change due to changing weather and climate conditions, which in turn may cause allergic reactions in human beings previously not exposed to specific types of pollen (D'Amato et al., 2007). For these reasons, there has been a growing interest in research of pollen in recent years.

Studies on pollen have started in the United States and Europe already in the 1960s. Niklas (1985) investigated pollen emission mechanisms. Potter and Cadman (2006) studied the relationship between pollen and allergic diseases. Other research dealt with the seasonal and regional dispersion of pollen (Damialis et al., 2005; Stach et al., 2007; Vázquez et al., 2003). Hjelmroos (1992), Mandrioli et al. (1984), Raynor et al. (1975) and Sofiev et al. (2006) studied the diffusion and long/short range transport of pollen on the basis of computer simulations. Raynor et al. (1974) investigated the transport and dispersion of pollen and the vertical distribution of pollen concentrations from their source regions along their transport path using an aircraft-mounted isokinetic sampler.

Pollen is injected into the air during the pollination period and can act as environmental pollutant by decreasing the visibility through scattering of sun light. One effect of the scattering of sun light by suspended airborne pollen is a corona that becomes visible around the sun. Parviainen et al. (1994) reported that coronas with a regular vertically-oriented elliptical shape were observed only on days with high pollen counts. Volz (1993) observed that the intensity of the corona increased during high pollen concentration in the atmosphere. Tränkle and Mielke (1994) showed with simulations that coronas may even be used as a simple indicator of the existence and the concentration of pollen because the shape of the corona is strongly correlated with the shape of the pollen.

Pollen can be an important source of natural aerosol pollution in the atmosphere during certain times of the year and specific regions on the globe, and can have considerable influence on the light scattering in the atmosphere during that time. However, there is only little literature available regarding the optical properties of pollen. Only Sassen (2008) reported on measurements of pollen in the lower atmosphere over Fairbanks (64.86°N, 147.84°W), Alaska. He found that tree pollen can generate a strong depolarization of laser-light emitted by a polarization lidar at 694 nm. Noh et al. (2012b) reports on the vertical distribution of pollen observed with lidar and the diffusion of pollen resulting from diurnal variations of the meteorological conditions (temperature, relative humidity, and wind speed).

In this contribution we report for the first time on pollen backscatter coefficients which were obtained by separating the pollen backscatter coefficients from the total aerosol backscatter coefficients using the lidar depolarization technique (Sakai et al., 2003; Sassen, 1977; Shimizu et al., 2004). The pollen-induced optical depth was inferred from the pollen backscatter coefficient, too. In addition, we investigated the effect of the observed pollen on some optical properties of the total atmospheric aerosols by comparing the results from our lidar observations to sun/sky radiometer measurements carried out at the lidar site.

Section 2 describes the instruments used in this study: pollen sampler, lidar and sun/sky radiometer, and the retrieval method of pollen optical depth. Section 3 presents the pollen optical depth. Section 4 discusses the effect of the pollen on optical properties of atmospheric aerosols. Section 5 contains the summary and conclusions.

2. Measurement and methodology

2.1. Pollen sampling

The pollen concentration was measured by the Burkard 7-Day Recording Volumetric Spore Sampler at the roof top of the Gwangju Bohoon hospital at an elevation of 216 m above sea level (asl). The building is located 1 km away from the lidar site. The spore sampler is normally used to monitor and analyze airborne biological particles. The performance of the standard spore sampler model is similar to the trap described by Hirst (1952). The Burkard trap sucks about 10 L of air per minute through a narrow, horizontal slit at the front of the sampling device. Behind the slit, inside the trap, a rotating drum is mounted. A sticky tape covers the drum, so that particles which are carried with the air through the slit stick to the tape. The effect of wind speed on the sampling efficiency is not known with high accuracy (Faegri et al., 1989). The sampling efficiency decreases for particle less than 5 μm in diameter (Willeke and Macher, 1999).

2.2. Depolarization lidar (DPL) system

The vertical distribution of the pollen was observed with the depolarization lidar system (DPL) of KOPRI (Korea Polar Research Institute) at the Gwangju Institute of Science & Technology (GIST) Gwangju, Korea (35.13°N, 126.50°E) at an elevation of 53 m asl from 5 to 7 May 2009. The DPL allowed us to measure vertical profiles of the linear volume (aerosol + molecule) depolarization ratio and the volume aerosol backscatter coefficient at 532 nm. The volume depolarization ratio is useful for identifying non-spherical particles, as for example mineral dust particles and biogenic pollen.

The light source of the DPL is a pulsed Nd:YAG laser that emits pulses at 532 nm wavelength with a power of 170 mJ. The pulse repetition rate is 30 Hz. The laser beam is expanded 5-fold using a beam expander which reduces the laser beam divergence to less than 0.2 mrad. The system has a coaxial configuration between receiver telescope and the laser beam. The backscattered light is collected with an 8 inch Schmidt–Cassegrain telescope. A polarizing beam splitter cube is used to separate the backscattered laser beam into its parallel and cross-polarized components. These two polarized beams are detected by photomultiplier tubes (PMT) which then transform the light pulses into electronic signals in the data acquisition system. An analog to digital converter (ADC) is used to digitize the output from the PMTs. The sampling rate is 60 MHz. Each measurement cycle consists of 3600 laser shots (2 min) that are used to produce vertical profiles with 2.5 m vertical resolution.

The linear volume depolarization ratio (δ) at 532 nm is obtained by taking the ratio of the total backscatter signals (from aerosols and molecules) that are linearly polarized with respect to the plane of polarization of the emitted laser to the total backscatter signals. In this paper we define δ as

$$\delta = \frac{P_s}{P_p + P_s} \quad (1)$$

The terms P_p and P_s are the backscatter signal intensities with respect to the parallel and the perpendicular plane of polarization of the outgoing laser beam. However, the total depolarization ratio depends on the concentration of aerosol particles. It decreases with decreasing aerosol particle concentration, as the depolarization effect from the molecules increases.

In order to estimate the contribution of the pollen to the total backscatter signals, the particle depolarization ratio (δ_p) is more appropriate. δ_p is estimated from the scattering ratio. We apply the equation used by Sakai et al. (2003):

$$\delta_p(z) = \frac{\delta(z)R(z) - \delta_m(z)}{R(z) - 1}. \quad (2)$$

The term $\delta(z)$ is the linear volume depolarization ratio at an altitude z . The expression δ_m describes the molecular depolarization ratio. We use 0.0049 in our study, see Sakai et al. (2003). $R(z)$ is the height-dependent scattering ratio. This scattering ratio can be written as $(\beta_a(z) + \beta_m(z))/\beta_m(z)$. The expression $\beta_a(z)$ describes the backscatter coefficient of the aerosol particles, and $\beta_m(z)$ describes the backscatter coefficient of the atmospheric molecules at altitude z .

The contribution ratio ($R_N(z)$) of the non-spherical particle backscattering coefficient to the total backscattering coefficient is calculated with Eq. (3) based on the method suggested by Shimizu et al. (2004). Shimizu et al. (2004) assume that there are only two aerosol types, i.e. non-spherical and spherical particles in an air mass. The authors furthermore assume that these two aerosol types are externally mixed. In this case, R_N can be expressed as

$$R_N(z) = \frac{(\delta_p(z) - \delta_2)(1 + \delta_1)}{(\delta_1 - \delta_2)(1 + \delta_p(z))}. \quad (3)$$

One part of δ_p describes the contribution by the non-spherical particles and another part of δ_p describes the contribution by the spherical particles, so we denote these two parts as δ_1 and δ_2 , respectively, for the external mixture. This ratio is sensitive to the selection of the values of δ_1 and δ_2 . The values of δ_1 and δ_2 can be empirically determined from lidar measurements. There are no measurements of depolarization ratios of pollen, therefore we assumed that the depolarization ratio is the same as that of mineral dust. We use for δ_1 and δ_2 the values 0.34 (pure dust) and 0.03 (urban haze), respectively, which follow from our previous long-

term lidar measurements (Noh et al., 2007, 2008, 2012a); note that similar values for the depolarization ratio were also measured for pure Saharan dust observed during the Saharan Mineral Dust Experiment (SAMUM) (Ansmann et al., 2011).

R_N from Eq. (3) can be caused by pollen and/or other non-spherical particles. In order to retrieve the contribution ratio of pollen (R_p) we need to remove the contribution by non-spherical particles other than that by pollen. R_p was retrieved by subtracting the contribution ratio of the non-spherical particles (R_a), which is measured during the pollen-free time at 07:00 local time (LT), see Section 3, Fig. 1(b), from the contribution ratio (R_N) according to Eq. (4):

$$R_p(z) = R_N(z) - R_a(z) \quad (4)$$

Finally, the pollen backscatter coefficient (β_p) was calculated by multiplying the aerosol backscatter coefficient (β_a) by R_p , i.e.,

$$\beta_p(z) = R_p(z)\beta_a(z) \quad (5)$$

The algorithm of Klett (1981, 1985) was used to retrieve the aerosol extinction and backscatter coefficients, respectively. In this method, the extinction-to-backscatter ratio (lidar ratio) has to be assumed. The lidar ratio was assumed height independent in our data analysis.

The pollen extinction coefficient was retrieved by multiplying β_p by the lidar ratio. However, there are no published values of the lidar ratio of biogenic pollen. The lidar ratio depends on many factors, such as the laser wavelength, the aerosol chemical composition, particle size distribution, and the aerosol index of refraction (Kovalev et al., 2004).

In our study we assumed a lidar ratio of 50 sr at 532 nm to retrieve the aerosol extinction coefficient (Murayama et al., 2001).

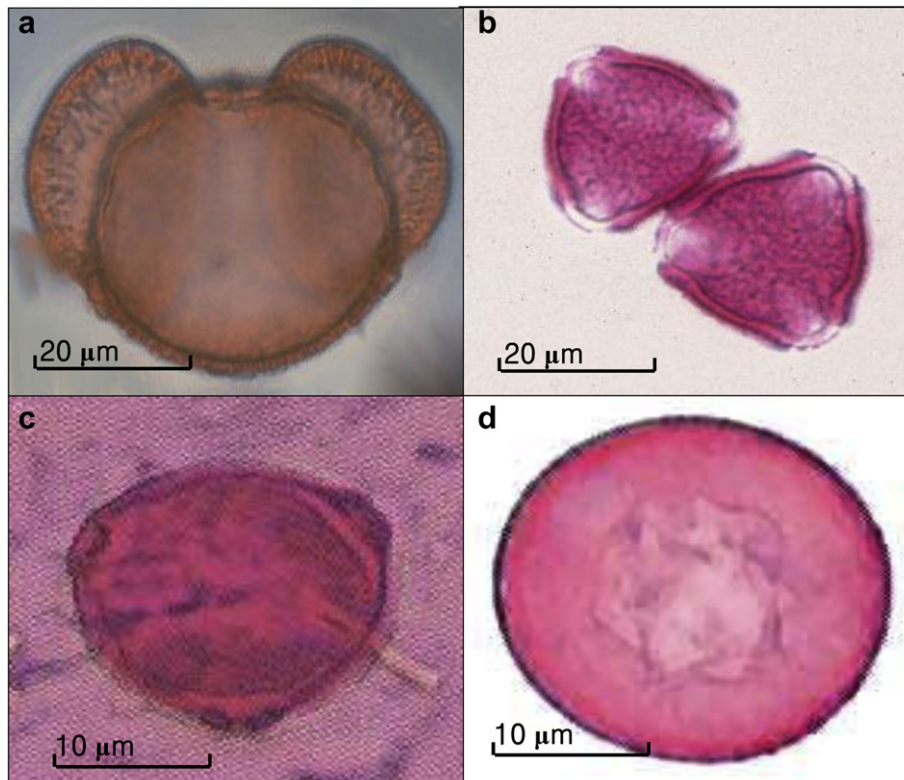


Fig. 1. Microphotographs of pollen grain observed in this study: (a) pine, (b) quercus, (c) betula, (d) juniper. Average size of pine, quercus, betula and juniper is 45–85, 28–38, 21–25, 20–30 μm , respectively.

A similar value can be taken as average lidar ratio for aerosol pollution in spring in our area, as shown by Noh et al. (2008). Highly polluted (light-absorbing) aerosols may show lidar ratios as high as 50–80 sr at 532 nm (e.g., Müller et al., 2007; Noh et al., 2011).

Cloud and marine particles are large, and correspondingly they have a small lidar ratio of around 20 sr (Ansmann et al., 2001, 1992; Doherty et al., 1999; Franke et al., 2001; Groß et al., 2011) at visible wavelengths.

Regarding the lidar ratio of pollen we assumed that it has values between that of clouds and moderately polluted particles (low light-absorption). We assumed a value between 35 and 45 sr to retrieve the pollen extinction coefficient. In this assumption we also considered that the particle lidar ratio decreases with increasing particles size (Kovalev et al., 2004).

2.3. AERONET sun/sky radiometer

Column-integrated spectral aerosol measurements were made with the polarized version of the CIMEL 318-1 Sun/sky radiometer (Holben et al., 1998) at the same site at which we carried out the lidar measurements. Aerosol optical depth ($\tau_{a,s}$) and the Ångström exponent (α) were retrieved using the AERONET algorithm (Dubovik and King, 2000). We analyzed the relationship between the pollen concentration (measured at ground) and the variation of aerosol optical depth. Detailed information on the cloud-screening and data-retrieval processes can be found in Dubovik and King (2000) and Smirnov et al. (2000). In our study we use level 2.0 data which can be downloaded from the AERONET site (<http://aeronet.gsfc.nasa.gov>).

3. Pollen optical depth

Table 1 shows the total and daily sorted pollen concentrations measured from 5 to 7 May 2009. A high pollen concentration between 1360 and 2696 $\text{m}^{-3} \text{day}^{-1}$ was observed during these three measurement days. The average concentration of pollen during the three days was 2002 $\text{m}^{-3} \text{day}^{-1}$. Fig. 1 shows micro-photographs of four major pollen species. Pine pollen which accounts for the highest concentration of pollen counted during the observation period shows an irregular shape due to the air bladders. Quercus pollen is almost triangular in shape.

Fig. 2 shows the vertical profiles of the aerosol backscatter coefficients (a) and the total volume depolarization ratio (b) measured by the DPL during the period of high pollen concentration. Fig. 2(a) shows that backscatter coefficients above 6 $\text{Mm}^{-1} \text{sr}^{-1}$ (at 532 nm) were continuously detected up to the top height of the PBL. The top height of the PBL varied between 1.5 and 2.0 km during the observational period. However, the variation of the linear volume depolarization ratio shows a different behavior than the variation of the backscatter coefficient.

Linear volume depolarization ratios less than 0.06 were observed during the night from 19:00 to 09:00 local time during all three nights. Linear volume depolarization ratios above 0.1 were only detected during daytime between 09:00 and 18:00 LT. Furthermore, this high linear volume depolarization ratio was only

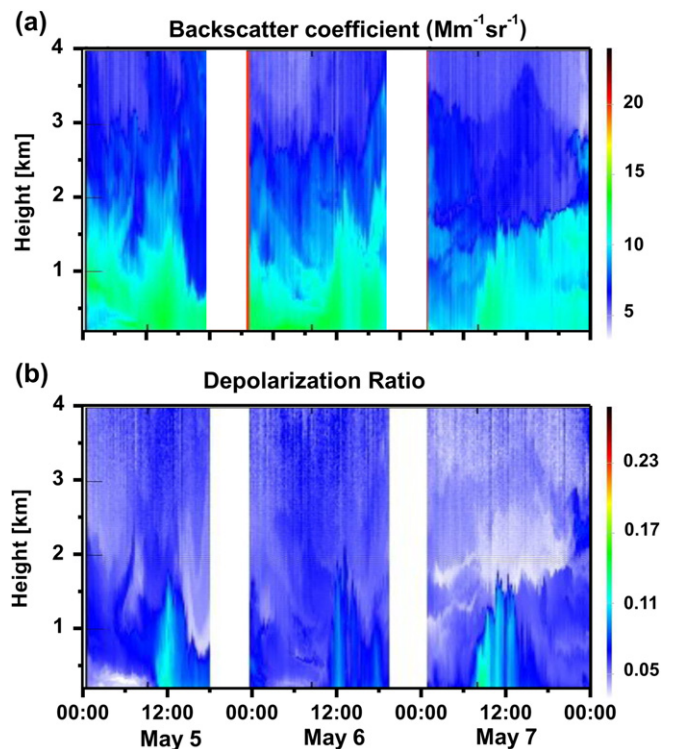


Fig. 2. Contour plots of backscatter coefficient (a) and linear volume depolarization ratio (b) measured by the depolarization lidar system from May 5 (00:00 LT) to May 7 (24:00 LT) 2009.

observed near the surface (200 m height above ground) around 09:00 LT. The altitude to which these high depolarization ratios were found increased gradually with time and reached the top of the PBL between 12:00 and 14:00 LT. After that time, the maximum height at which these depolarization ratios were detected gradually decreased again. This phenomenon repeated during the three days of lidar observations. We conclude that this pattern of the changing depolarization ratio from low to high values with height during daytime was induced by the increase of the concentration of non-spherical pollen particles in the atmosphere. Details can be found in Noh et al. (2012b).

Fig. 3 shows hourly values of the total aerosol backscatter coefficient and the pollen-only backscatter coefficient calculated from Eqs. (3–5). The results are given for the time from 09:00 to 17:00 LT on 5, 6, and 7 May 2009. The pollen backscatter coefficient gradually increases with time and reaches its maximum around noon time. The maximum altitude of significant values of the pollen backscatter coefficient is at 1.8 km at that time. This pattern of the backscatter coefficient indicates that pollen particles that are released from trees into the air can be dispersed within the planetary boundary layer by the effect of small scale convection, updrafts and downdrafts in the urban PBL and gravity if proper meteorological conditions like high temperature and wind speed and low relative humidity prevail Noh et al. (2012b).

Fig. 4 shows hourly-averaged aerosol optical depth (τ_a), and pollen optical depth (τ_p) at 532 nm from 5 to 7 May. τ_a and τ_p are calculated by integrating the extinction coefficients of the total aerosol load and the contribution from the pollen, respectively. For that purpose we multiplied the backscatter coefficients shown in Fig. 2(a) with lidar ratios of 50 sr for the aerosols. Lidar ratios between 35 and 45 sr were used to retrieve the extinction coefficients of pollen, respectively. τ_p was calculated by integrating the average values of the pollen extinction coefficients according to the different lidar ratios.

Table 1
Pollen concentrations during the intensive observation period.

Date (2009 May)	Total ($\# \text{m}^{-3}$)	Pine ($\# \text{m}^{-3}$)	Quercus ($\# \text{m}^{-3}$)	Betula ($\# \text{m}^{-3}$)	Juniper ($\# \text{m}^{-3}$)	Etc ($\# \text{m}^{-3}$)
5th	1360	582	96	0	0	682
6th	2696	1086	253	1	6	1350
7th	1952	868	100	4	4	976
Average	2002	845	150	1.7	3.3	1003

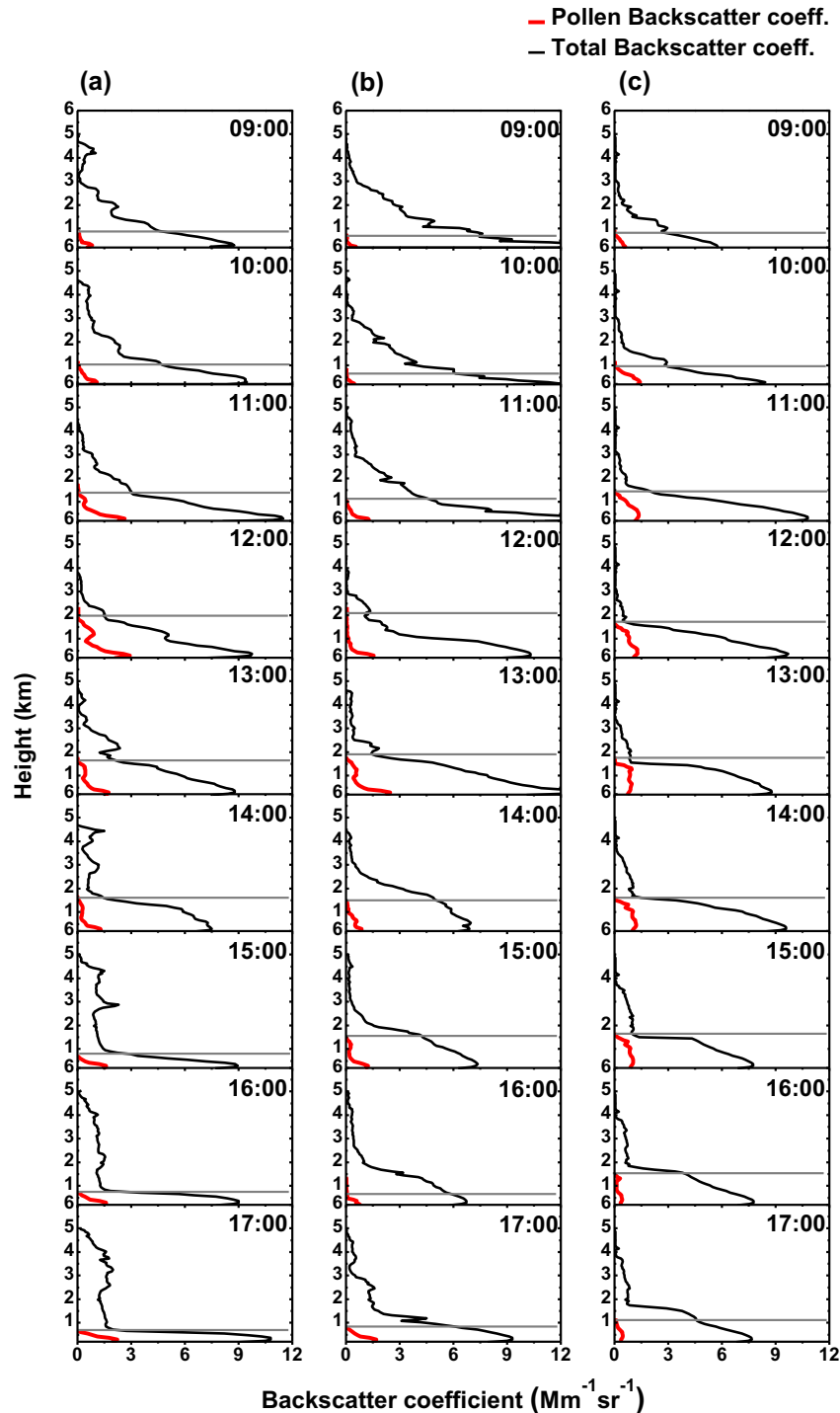


Fig. 3. Vertical profiles of aerosol backscatter coefficient (black line) and pollen backscatter coefficient (red line). Gray-colored horizontal lines indicate the maximum height of the pollen plume on the basis of the pollen backscatter coefficient. (For interpretation of the references to color in this figure legend, the reader is referred to the web version of this article.)

τ_a shows high values between 0.4 and 0.6 on 5 and 6 May whereas relatively low values of 0.2–0.3 were measured on 7 May. τ_p shows the same diurnal pattern which can also be seen for the volume depolarization ratio, see Fig. 2(b). τ_p increases gradually during the daytime and then reaches its maximum value of 0.14 and 0.10 on 5 and 6 May, respectively, at 13:00 LT. Values around 0.10 were observed from 11:00 to 15:00 LT on 7 May.

Average values of hourly τ_p were 0.062 ± 0.037 , 0.041 ± 0.028 , and 0.067 ± 0.036 on 5, 6, and 7 May, respectively. These values do

not show a significant correlation with the pollen concentrations (see Table 1) measured on each day. The highest pollen concentration of 2696 m^{-3} was counted on 6 May. At that time a low value of 0.041 ± 0.028 was recorded for τ_p . On the contrary, a high value of τ_p was measured during comparably low pollen concentrations of 1360 m^{-3} on 5 May.

τ_p was derived from the lidar measurements which contain information on the vertical distribution of the pollen in the atmosphere. In contrast, the pollen concentration in the study of the

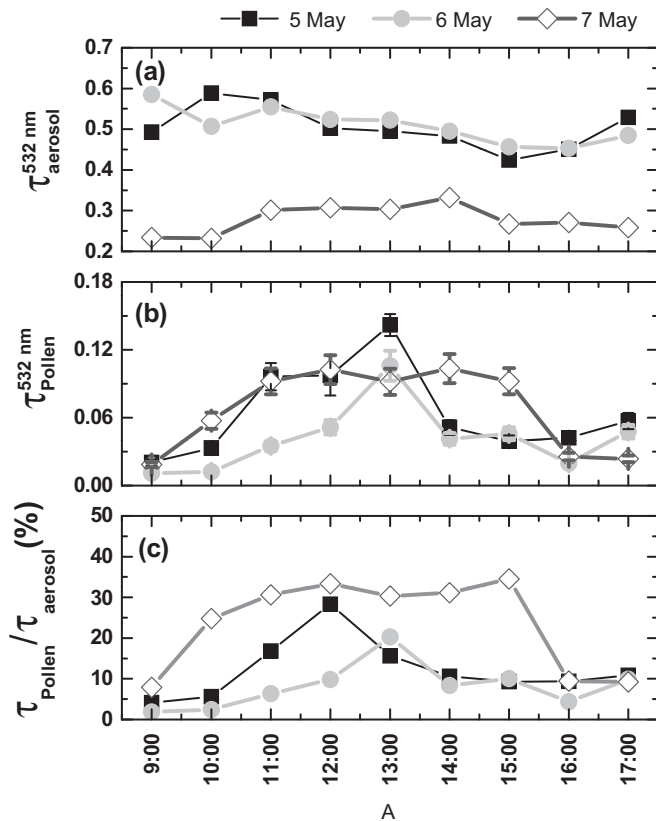


Fig. 4. Aerosol optical depth (a), pollen optical depth (b) and the ratio of pollen optical depth to aerosol optical depth at 532 nm. Error bars of the pollen optical depth denote the standard deviation of pollen optical depth computed from the different lidar ratio values (35 to 45 sr) we used in our study.

Korea Meteorological Administration (KMA) only describes the variations of the pollen concentration near the surface. We assume that the variation of τ_p was affected by other parameters that did not affect the concentrations measured on the surface.

The release, dispersal and transport of pollen are influenced by several meteorological factors, such as rainfall, air temperature, relative humidity, and wind speed (Adams-Groom et al., 2002; Alba et al., 2000; Bartková-Ščevková, 2003; Gilissen, 1977; Gioulekas et al., 2003; Vázquez et al., 2003). Bartková-Ščevková (2003) and Norris-Hill and Emberlin (1991) reported that daily temperature and relative humidity are significant factors that influence the release of pollen grains in the atmosphere. Niklas (1985) reported that relative humidity influences not only the extent to which individual pollen grains dehydrate, but also the extent to which pollen is released, thereby affecting airborne pollen concentrations. Durham (1943) also reported that low humidity conditions affect the diffusion of pollen in the atmosphere by decreasing the specific gravity of pollen grains which thus influences their ability to settle to the ground, which may in turn lead to higher optical depths compared to more humid conditions. Latorre and Caccavari (2009) showed that there is a significant positive correlation with temperature and wind speed and a negative correlation with relative humidity of the total pollen concentration.

Fig. 5 shows hourly values of the variation of wind speed, relative humidity, and temperature from 00:00 LT on 5 May to 24:00 LT on 7 May. During these 3 days, the hourly-averaged maximum temperature was reached between 12:00 and 14:00 LT, whereas relative humidity reached its minimum. Wind speed showed a similar pattern like the variation of temperature, i.e. the maximum around noon and the minimum at night time. Alba et al.

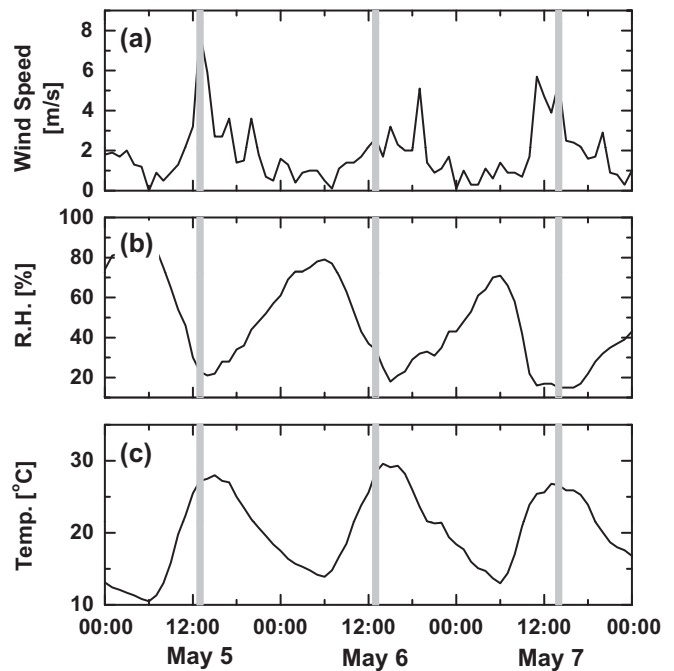


Fig. 5. Hourly-averaged meteorological data observed from 00:00 LT on May 5 to 24:00 LT on May 7, 2009. Shown are (a) wind speed, (b) relative humidity, and (c) temperature. Gray-colored vertical lines denote time of the maximum pollen optical depth on each day.

(2000), Jato et al. (2000), Käpylä (1984) and Bartková-Ščevková (2003) found that the temperature, the duration of the sunshine, and the wind speed positively affect the concentration of pollen, i.e., lead to an increase of the pollen concentration. Alternatively, rainfall and humidity during pollination periods tend to decrease pollen concentrations. In the present study, when temperature and humidity met these pollen-releasing conditions, pollen concentration increased, as shown in Fig. 3, thereby inducing depolarization scattering by the non-spherical shapes of pollen (Noh et al., 2012b).

Wind-pollinated plants can produce millions of pollen grains each year if favorable meteorological conditions are met. However, most of the pollen grains injected into the air will settle close to their sources, respectively, and only a few will be diffused over longer distances. Gregory (1978) reports that only about 10% of the total number of pollen grains can be diffused over larger distances. Although temperature and relative humidity strongly affect pollen release, wind speed can be considered as the most dominant parameter that has direct influence on the diffusion of pollen in the atmosphere.

A positive dependence on temperature and a negative dependence on relative humidity of the pollen optical depth can be seen in Fig. 6 (red lines). The correlation itself however is negligible, which in part may be the result of our sparse data set and the uncertainties involved in our data analysis. Temperature and relative humidity also show similar maximum and minimum values around noon time during the 3 days regardless of the time of maximum pollen optical depth. In contrast, average wind speed varied from 3.5 to 2.1 to 3.1 m s^{-1} on 5, 6, and 7 May, respectively, see Fig. 5. The variations of wind speed match the variation of τ_p as shown in Fig. 4(b). We also find a positive correlation of pollen optical depth with wind speed.

Fig. 7 shows the relationship between wind speed and pollen optical depth. The correlation coefficient is 0.5 when we consider all data collected during the 3 observation days. The highest pollen

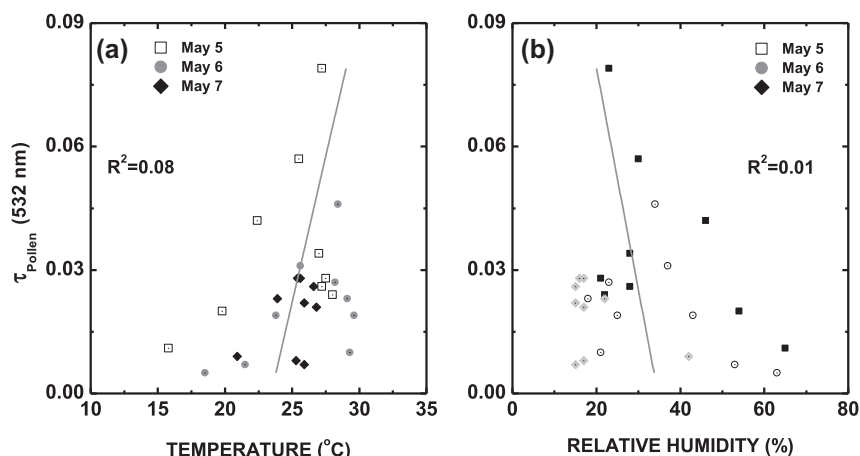


Fig. 6. Correlation plots of pollen optical depth versus temperature (a) and versus relative humidity (b).

optical depth of 0.142 was measured when the maximum wind speed of 7.9 m s^{-1} was recorded at 13:00 LT on 5 May.

We can estimate the minimum and maximum pollen optical depth from the prevailing wind speed. We find a rather broad variation of pollen optical depth for wind speeds as high as 3 m s^{-1} . The comparably strong correlation of 0.5 is mainly caused by the data points that include wind speeds above 4 m s^{-1} . We note that our data base is certainly too sparse to allow for a generalization of the relationship between pollen optical depth and wind speed, in particular as we have no information on the concentration of the investigated pollen at their sources and no information on the urban climate. The latter point would call for detailed micro-meteorological studies for which we do not have the appropriate measurement instruments. Nevertheless this plot shows a possible scenario of pollen optical depth in dependence of wind speed.

4. Influence of pollen on the variation of optical properties of aerosols

The variation of some aerosol optical properties induced by pollen was investigated by comparing lidar data and sun/sky radiometer data. Fig. 8 shows hourly variations of aerosol optical depth $\tau_{\text{a,s}}$ at 440 nm and the Ångström exponent α (440–870 nm wavelength range) measured by sun/sky radiometer during the same

period the lidar measurements were carried out. The variation of $\tau_{\text{a,s}}$ shows a similar pattern like the lidar-derived τ_{a} , see Fig. 4(a). $\tau_{\text{a,s}}$ varied from 0.4 to 0.6 on 5 and 6 May and between 0.2 and 0.3 on 7 May. α varied between 1.1 and 1.4. Lower values than the average values were observed between 10:00 and 14:00 LT on each day. During that time we found a relatively high τ_{p} which indicates a high pollen concentration during this time.

Fig. 9 shows the diurnal variability of $\tau_{\text{a,s}}$ and α measured by sun/sky radiometer in terms of change of the hourly mean values (given in percent). We separated the data into the pollen period (5, 6, 7 May), and the spring period in which no pollen and no Asian dust were recorded. This period refers to the time frame between March and May 2009. There are virtually no changes of $\tau_{\text{a,s}}$ during the spring period during daytime. The increasing trend is clearly seen during the pollen period that occurred between 10:00 and 13:00 LT, see Fig. 8(b). The pattern of increasing $\tau_{\text{a,s}}$ during midday is consistent with the variability of pollen optical depth, as shown in Fig. 4(b).

There are comparably small changes of the diurnal variation of α in spring, see Fig. 8(a). However, α decreased during the pollen period while $\tau_{\text{a,s}}$ increased during this same period. It means that the concentration of particles of large size increased during that time. The size of pollen is in the range of 20–100 μm which is usually significantly larger than the size of most other atmospheric aerosols, except for dust, which may reach similar

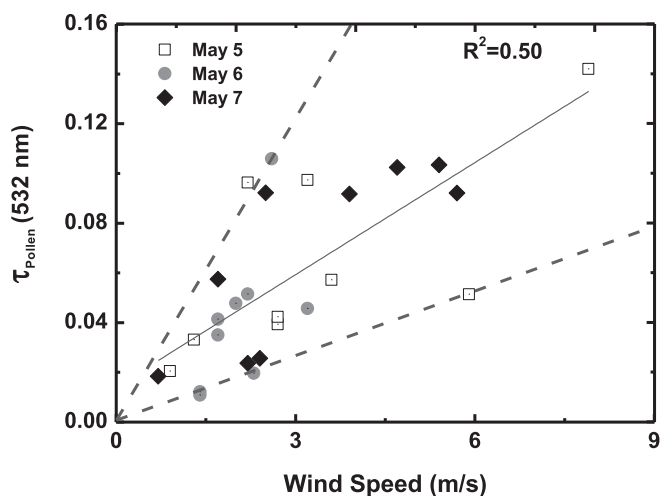


Fig. 7. Dependence of pollen optical depth on wind speed. The dashed lines denote the possible minimum and maximum pollen optical depth for given wind speed.

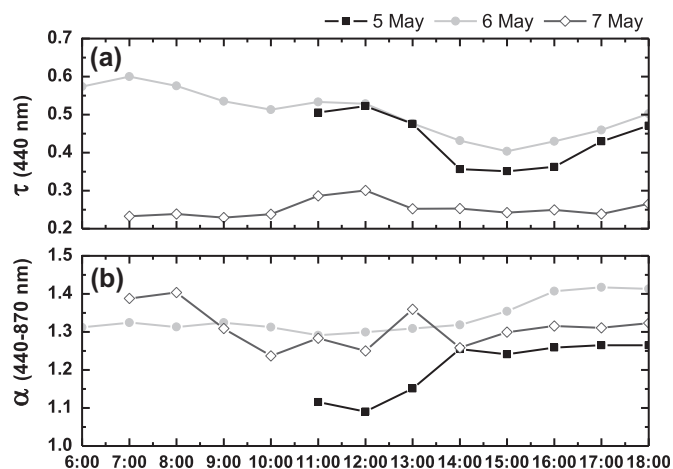


Fig. 8. Aerosol optical depth at 440 nm (a) and Ångström exponent between 440 and 870 nm (b) measured by sun/sky radiometer.

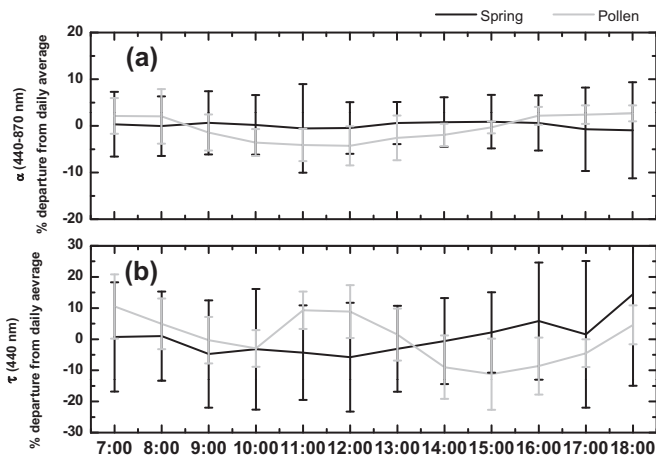


Fig. 9. Diurnal variability of aerosol optical depth at 440 nm (a) and Ångström exponent between 440 and 870 nm (b).

size, but transport distance and the duration such large dust grains remain airborne is restricted by sedimentation processes and wind speed. We believe that the meteorological situation favored the emission of a large amount of pollen particles which lead to an increase of $\tau_{a,s}$ and the decrease of α .

5. Conclusions

For the first time, several optical properties, i.e. backscatter coefficients, extinction coefficients and optical depth of biogenic pollen were retrieved by lidar measurements. The variation of aerosol optical properties by pollen in the atmosphere was also investigated by comparing lidar and sun/sky radiometer data.

The average hourly-values of τ_p retrieved from the depolarization lidar were 0.036 ± 0.021 , 0.021 ± 0.013 , and 0.019 ± 0.008 at 532 nm, when the pollen concentration was 1360, 2696, and 1952 m^{-3} on 5, 6, and 7 May 2009, respectively. The ratio of pollen optical depth to total aerosol optical depth was 2–34%. The highest ratio was observed around noon time on each day. We find a positive correlation between τ_p and wind speed. Pollen particles were mainly detected during daytime, which resulted in the increase of aerosol optical depth and the decrease of the Ångström exponent.

From these results, we conclude that pollen can act as one important natural source of atmospheric particles during periods of strong pollen emission. We assume that there are strong pollen emissions in the boreal areas of the northern hemisphere (Alaska, Canada, and Siberia) during the onset of the growth season in spring, which may have significant effects on atmospheric optical properties. Although our observations certainly reflect only a minor part of the overall large-scale effect of pollen during the growth season, the results point to the significance of pollen emissions. It may be useful to investigate in the future vertical profiles of heating rates exerted by pollen during the growth season in these areas.

The diurnal pattern of pollen optical depth that we found in this study can serve as useful information to estimate the effect of pollen to total aerosol optical properties retrieved by space-borne sensors such as the Cloud-Aerosol Lidar and Infrared Pathfinder Satellite Observations (CALIPSO), as well as passive sensors which do not have any aerosol model of pollen in their data analysis algorithms. Also, the information about the diurnal pattern and the vertical distribution of pollen can be helpful in protecting public health on the basis of a higher accuracy of pollen forecasts in urban areas.

Acknowledgment

This work was supported by the National Research Foundation of Korea (NRF) grant funded by the Korea government (MEST) (No. 2012R1A1A2002983). This work was partly supported by the project “Reconstruction and observation of components for the Southern and Northern Annular Mode to investigate the cause of polar climate change (PE12010)” of the Korea Polar Research Institute.

References

- Adams-Groom, B., Emberlin, J., Corden, J., Millington, W., Mullins, J., 2002. Predicting the start of the birch pollen season at London, Derby and Cardiff, United Kingdom, using a multiple regression model, based on data from 1987 to 1997. *Aerobiologia* 18, 117–123.
- Alba, F., De La Guardia, C.D., Comtois, P., 2000. The effect of meteorological parameters on diurnal patterns of airborne olive pollen concentration. *Grana* 39, 200–208.
- Ansmann, A., Wandinger, U., Riebesell, M., Weitkamp, C., Michaelis, W., 1992. Independent measurement of extinction and backscatter profiles in cirrus clouds by using a combined Raman elastic-backscatter lidar. *Applied Optics* 31, 7113–7131.
- Ansmann, A., Wagner, F., Althausen, D., Müller, D., Herber, A., Wandinger, U., 2001. European pollution outbreaks during ACE 2: lofted aerosol plumes observed with Raman lidar at the Portuguese coast. *Journal of Geophysical Research* 106, 20725–20733.
- Ansmann, A., Petzold, A., Kandler, K., Tegen, I., Wendisch, M., Müller, D., Weinzierl, B., Müller, T., Heintzenberg, J., 2011. Saharan Mineral Dust Experiments SAMUM-1 and SAMUM-2: what have we learned? *Tellus B* 63, 403–429.
- Bartková-Ščevková, J., 2003. The influence of temperature, relative humidity and rainfall on the occurrence of pollen allergens (*Betula*, *Poaceae*, *Ambrosia artemisiifolia*) in the atmosphere of Bratislava (Slovakia). *International Journal of Biometeorology* 48, 1–5.
- Beggs, P., 2004. Impacts of climate change on aeroallergens: past and future. *Clinical & Experimental Allergy* 34, 1507–1513.
- D’Amato, G., Cecchi, L., Bonini, S., Nunes, C., Annesi-Maesano, I., Behrendt, H., Liccardi, G., Popov, T., Van Cauwenberge, P., 2007. Allergenic pollen and pollen allergy in Europe. *Allergy* 62, 976–990.
- D’Amato, G., Cecchi, L., 2008. Effects of climate change on environmental factors in respiratory allergic diseases. *Clinical & Experimental Allergy* 38, 1264–1274.
- Damialis, A., Gioulekas, D., Lazopoulou, C., Balafoutis, C., Vokou, D., 2005. Transport of airborne pollen into the city of Thessaloniki: the effects of wind direction, speed and persistence. *International Journal of Biometeorology* 49, 139–145.
- Doherty, S.J., Anderson, T.L., Charlson, R.J., 1999. Measurement of the lidar ratio for atmospheric aerosols with a 180 backscatter nephelometer. *Applied Optics* 38, 1823–1832.
- Dubovik, O., King, M.D., 2000. A flexible inversion algorithm for retrieval of aerosol optical properties from sun and sky radiance measurements. *Journal of Geophysical Research* 105, 20673–20696.
- Durham, O.C., 1943. The volumetric incidence of atmospheric allergens: I. Specific gravity of pollen grains. *Journal of Allergy* 14, 455–461.
- Esch, R., Bush, R.K., 2003. Aerobiology of outdoor allergens. In: Middleton’s Allergy: Principles and Practice, sixth ed. Mosby, Philadelphia, pp. 529–555.
- Faegri, K., Iversen, J., Kaland, P., Krzywinski, K., 1989. *Textbook of Pollen Analysis*. Wiley, New York, USA.
- Franke, K., Ansmann, A., Müller, D., Althausen, D., Wagner, F., Scheele, R., 2001. One-year observations of particle lidar ratio over the tropical Indian Ocean with Raman lidar. *Geophysical Research Letters* 28, 4559–4562.
- Frei, T., 1998. The effects of climate change in Switzerland 1969–1996 on airborne pollen quantities from hazel, birch and grass. *Grana* 37, 172–179.
- Gilissen, L., 1977. The influence of relative humidity on the swelling of pollen grains in vitro. *Planta* 137, 299–301.
- Gioulekas, D., Damialis, A., Papakosta, D., Syrigou, A., Mpaka, G., Saxoni, F., Patakas, D., 2003. 15-year aeroallergen records. Their usefulness in Athens Olympics, 2004. *Allergy* 58, 933–938.
- Gregory, P., 1978. Distribution of airborne pollen and spores and their long distance transport. *Pure and Applied Geophysics* 116, 309–315.
- Groß, S., Tesche, M., Freudenthaler, V., Toledano, C., Wiegner, M., Ansmann, A., Althausen, D., Seefeldner, M., 2011. Characterization of Saharan dust, marine aerosols and mixtures of biomass-burning aerosols and dust by means of multi-wavelength depolarization and Raman lidar measurements during SAMUM 2. *Tellus B* 63, 706–724.
- Hirst, J., 1952. An automatic volumetric spore trap. *Annals of Applied Biology* 39, 257–265.
- Hjelmroos, M., 1992. Long-distance transport of betula pollen grains and allergic symptoms. *Aerobiologia* 8, 231–236.
- Holben, B., Eck, T., Slutsker, I., Tanre, D., Buis, J., Setzer, A., Vermote, E., Reagan, J., Kaufman, Y., Nakajima, T., 1998. AERONET—a federated instrument network and data archive for aerosol characterization. *Remote Sensing of Environment* 66, 1–16.
- Jato, M., Frenguelli, G., Rodriguez, F., Aira, M., 2000. Temperature requirements of *Alnus* pollen in Spain and Italy (1994–1998). *Grana* 39, 240–245.

- Käpylä, M., 1984. Diurnal variation of tree pollen in the air in Finland. *Grana* 23, 167–176.
- Klett, J.D., 1981. Stable analytical inversion solution for processing lidar returns. *Applied Optics* 20, 211–220.
- Klett, J.D., 1985. Lidar inversion with variable backscatter/extinction ratios. *Applied Optics* 24, 1638–1643.
- Kovalev, V.A., Eichinger, W.E., Wiley, J., 2004. *Elastic Lidar: Theory, Practice, and Analysis Methods*. Wiley-Interscience.
- Latorre, F., Caccavari, M.A., 2009. Airborne pollen patterns in Mar del Plata atmosphere (Argentina) and its relationship with meteorological conditions. *Aerobiologia* 25, 297–312.
- Mandrioli, P., Negrini, M.G., Cesari, G., Morgan, G., 1984. Evidence for long range transport of biological and anthropogenic aerosol particles in the atmosphere. *Grana* 23, 43–53.
- Müller, D., Ansmann, A., Mattis, I., Tesche, M., Wandinger, U., Althausen, D., Pisani, G., 2007. Aerosol-type-dependent lidar ratios observed with Raman lidar. *Journal of Geophysical Research* 112, D16202.
- Murayama, T., Sugimoto, N., Uno, I., Kinoshita, K., Aoki, K., Hagiwara, N., Liu, Z., Matsui, I., Sakai, T., Shibata, T., 2001. Ground-based network observation of Asian dust events of April 1998 in east Asia. *Journal of Geophysical Research* 106, 18345–18360.
- Niklas, K.J., 1985. The aerodynamics of wind pollination. *The Botanical Review* 51, 328–386.
- Noh, Y.M., Kim, Y.J., Choi, B.C., Murayama, T., 2007. Aerosol lidar ratio characteristics measured by a multi-wavelength Raman lidar system at Anmyeon Island, Korea. *Atmospheric Research* 86, 76–87.
- Noh, Y.M., Kim, Y.J., Müller, D., 2008. Seasonal characteristics of lidar ratios measured with a Raman lidar at Gwangju, Korea in spring and autumn. *Atmospheric Environment* 42, 2208–2224.
- Noh, Y.M., Müller, D., Mattis, I., Lee, H., Kim, Y.J., 2011. Vertically resolved light-absorption characteristics and the influence of relative humidity on particle properties: multiwavelength Raman lidar observations of East Asian aerosol types over Korea. *Journal of Geophysical Research* 116, D06206.
- Noh, Y.M., Müller, D., Lee, H., Lee, K.H., Kim, K., Shin, S., Kim, Y.J., 2012a. Estimation of radiative forcing by the dust and non-dust content in mixed east Asian pollution plumes on the basis of depolarization ratios measured with lidar. *Atmospheric Environment* 61, 221–231.
- Noh, Y.M., Mueller, D., Lee, H., Lee, K., Shin, D., Shin, S., Choi, T.J., Choi, Y.J., Kim, K.R., 2012b. Investigation of diurnal patterns in vertical distributions of pollen in the lower troposphere using LIDAR technique. *Atmospheric Chemistry and Physics Discussion* 12, 31187–31204.
- Norris-Hill, J., Emberlin, J., 1991. Diurnal variation of pollen concentration in the air of north-central London. *Grana* 30, 229–234.
- Parviainen, P., Bohren, C.F., Mäkelä, V., 1994. Vertical elliptical coronas caused by pollen. *Applied Optics* 33, 4548–4551.
- Potter, P., Cadman, A., 2006. Pollen allergy in South Africa. *Clinical & Experimental Allergy* 26, 1347–1354.
- Raynor, G.S., Hayes, J.V., Ogden, E.C., 1974. Mesoscale transport and dispersion of airborne pollens. *Journal of Applied Meteorology* 13, 87–95.
- Raynor, G.S., Hayes, J.V., Ogden, E.C., 1975. Particulate dispersion from sources within a forest. *Boundary-Layer Meteorology* 9, 257–277.
- Sakai, T., Nagai, T., Nakazato, M., Mano, Y., Matsumura, T., 2003. Ice clouds and Asian dust studied with lidar measurements of particle extinction-to-backscatter ratio, particle depolarization, and water-vapor mixing ratio over Tsukuba. *Applied Optics* 42, 7103–7116.
- Sassen, K., 1977. Optical backscattering from near-spherical water, ice, and mixed phase drops. *Applied Optics* 16, 1332–1341.
- Sassen, K., 2008. Boreal tree pollen sensed by polarization lidar: depolarizing biogenic chaff. *Geophysical Research Letters* 35, L18810.
- Shea, K.M., Truckner, R.T., Weber, R.W., Peden, D.B., 2008. Climate change and allergic disease. *Journal of Allergy and Clinical Immunology* 122, 443–453.
- Shimizu, A., Sugimoto, N., Matsui, I., Arao, K., Uno, I., Murayama, T., Kagawa, N., Aoki, K., Uchiyama, A., Yamazaki, A., 2004. Continuous observations of Asian dust and other aerosols by polarization lidars in China and Japan during ACE-Asia. *Journal of Geophysical Research* 109, D19S17.
- Smirnov, A., Holben, B., Eck, T., Dubovik, O., Slutsker, I., 2000. Cloud-screening and quality control algorithms for the AERONET database. *Remote Sensing of Environment* 73, 337–349.
- Sofiev, M., Siljamo, P., Ranta, H., Rantio-Lehtimäki, A., 2006. Towards numerical forecasting of long-range air transport of birch pollen: theoretical considerations and a feasibility study. *International Journal of Biometeorology* 50, 392–402.
- Stach, A., Smith, M., Skjuth, C., Brandt, J., 2007. Examining Ambrosia pollen episodes at Poznań (Poland) using back-trajectory analysis. *International Journal of Biometeorology* 51, 275–286.
- Teranishi, H., Kenda, Y., Katoh, T., Kasuya, M., Oura, E., Taira, H., 2000. Possible role of climate change in the pollen scatter of Japanese cedar *Cryptomeria japonica* in Japan. *Climate Research* 14, 65–70.
- Tränkle, E., Mielke, B., 1994. Simulation and analysis of pollen coronas. *Applied Optics* 33, 4552–4562.
- Vázquez, L., Galán, C., Domínguez-Vilches, E., 2003. Influence of meteorological parameters on olea pollen concentrations in Córdoba (South-western Spain). *International Journal of Biometeorology* 48, 83–90.
- Volz, F.E., 1993. Scattering functions near the Sun by large aerosols. *Applied Optics* 32, 2773–2779.
- Willeke, K., Macher, J., 1999. Air Sampling. *Bioaerosols: Assessments and Control*, pp. 11.11–11.25.